Supplementary information

for M.G. Düser et al. "36° step size of proton-driven *c*-ring rotation in F_oF_1-ATP synthase"

1. Setup for duty cycle-optimized alternating laser excitation (DCO-ALEX)

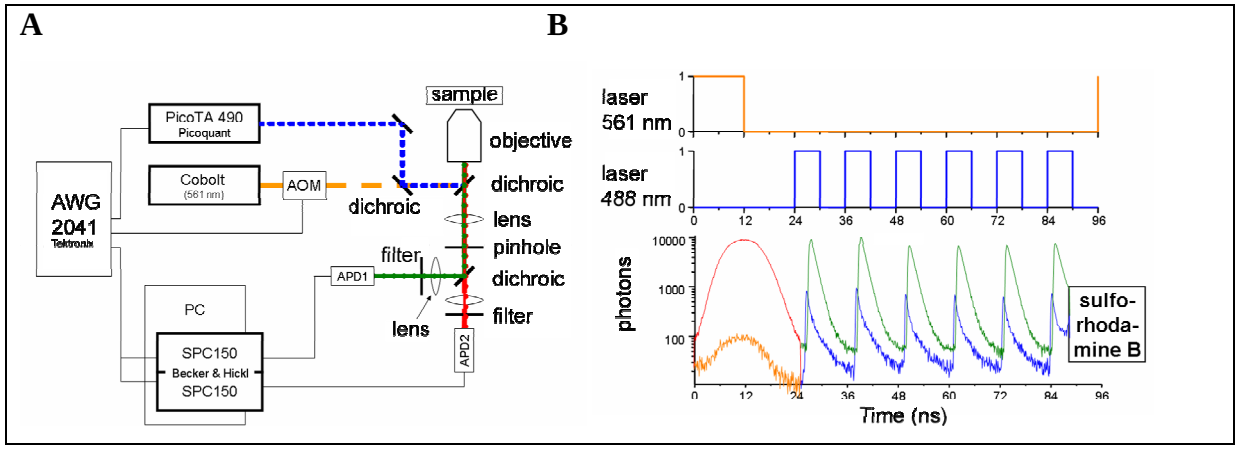

Figure S1: Setup for confocal single-molecule FRET with duty cycle-optimized alternating laser excitation. **A**, triggering the two lasers by an arbitrary waveform generator for direct pulsing the 488 nm laser and switching of the 561 nm laser *via* an acousto-optical modulator. **B**, pulse sequence with one 561 nm pulse for direct excitation of the FRET acceptor Alexa568 and six subsequent 488 nm pulses for time-resolved FRET (EGFP and Alexa568).

2. Fluorescence anisotropy measurements with single F_oF_1-ATP synthase

Fluorescence anisotropies of single EGFP-*a*-F_oF_1 (linear polarized excitation with 488 nm) or Alexa568-*c*-F_oF_1 (linear polarized excitation with 561 nm; continuous-wave laser Jive, Cobolt) in liposomes were measured separately in the confocal microscope using a polarizing beamsplitter in the fluorescence pathway. Signals of the two APDs were recorded by two synchronized TCSPC cards (SPC152, Becker&Hickl, Germany). Intensity thresholds of at least 40 counts/ms and maximum 150 counts/ms were applied to identify photon bursts of single F_oF_1-ATP synthases. Fluorescence anisotropy values were calculated for each burst after correction for the APD detection efficiencies. Aqueous solutions of rhodamine 110, erythrosine blue, sulforhodamine B (SRB) and rhodamine 101 in water were used as anisotropy reference dyes. In Fig. S2, single EGFP-*a*-F_oF_1 ATP synthases show a static fluorescence anisotropy of r=0.29±0.13 (mean and standard deviation σ, measured for 184 F_oF_1) as expected for the autofluorescent protein. However, fusing EGFP to the C terminus of the *a* subunit did not increase the anisotropy further. The static anisotropy of single Alexa568-*c*-F_oF_1 ATP was r=0.22±0.1 in 658 molecules indicating a restricted mobility. Taking both fluorophore anisotropies into account, the error for the FRET distance measurements can be

calculated to be smaller than 20% (Dale et al, 1979). This is in good agreement with the mean 0.5 nm distance error broadening, which was required to simulate the FRET distance change histograms (see Fig. 4 in the manuscript).

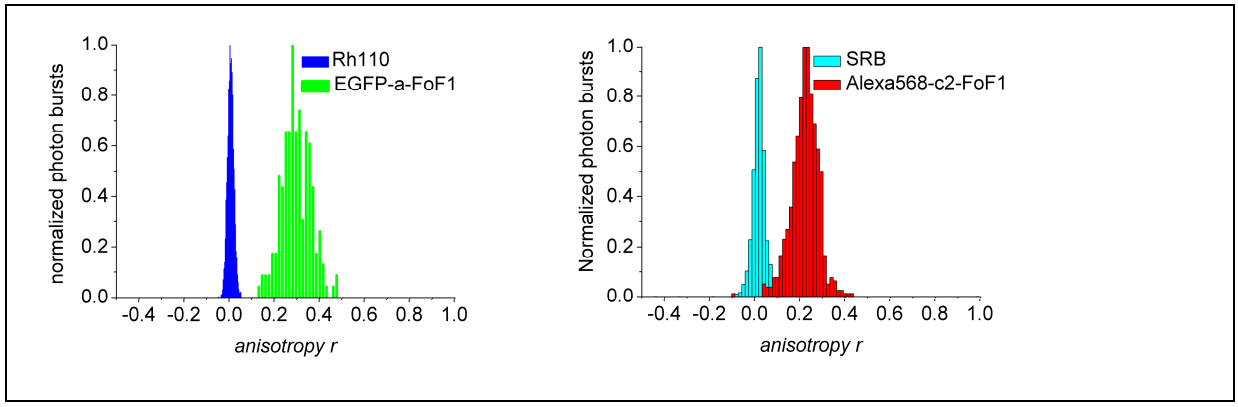

Figure S2: Fluorescence anisotropies of single EGFP-*a*-F_oF_1 or Alexa568-*c*-F_oF_1 in liposomes and of the free reference dyes rhodamine 110 and sulforhodamine B.

3. FRET distance analysis

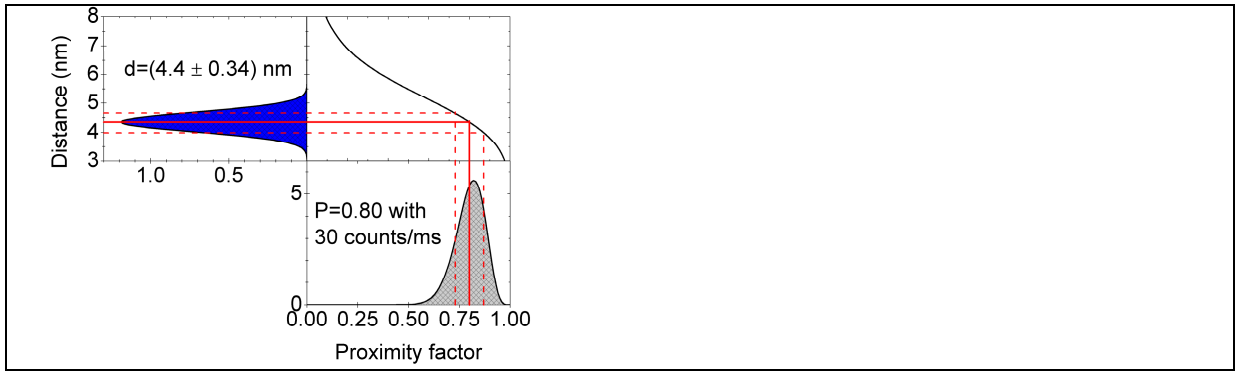

Figure S3: Example for time bin with a proximity factor of P=0.80 and a total count rate of 30 counts per ms. Bottom, corresponding Beta distribution with the borders P_1 and P_2; top right, transfer function *d=f(p)* to transform the proximity factor into an absolute distance; top left, Gaussian distribution around the calculated distance of 4.4 nm and a 2σ-value of 0.67 nm given by the limited count rate of 30 counts per ms. These borders P_1 and P_2 are transformed into distances d_1 and d_2; in the same way as the proximity factor P. These new distance borders are approximately symmetrically distributed around the distance d itself. Thus, the distance is visualized as a Gaussian with mean d and an averaged standard deviation from d_1 to d_2.

4. EGFP fluorescence lifetime analysis

The EGFP fluorescence lifetimes per FRET level were plotted against the EGFP / Alexa568 intensity ratio (Antonik et al, 2006) to prove that the intensity ratio corresponds to FRET (Fig. S4).

Figure S4: EGFP fluorescence lifetime in 641 FRET levels found in 180 F_oF_1-ATP synthases during ATP synthesis. The intensity ratio I_D/D_A for EGFP (I_D) and Alexa568 (I_A) corresponds to the FRET efficiency, and the EGFP lifetime in each FRET level clearly depends on FRET to Alexa568 at *c*. The black curve is defined by the relation of both intensity ratio and donor lifetime to FRET efficiency.

5. FRET transition density plot and dwell time histograms for ATP hydrolysis and in the presence of aurovertin B

After assigning the FRET levels, the intermediary levels - but not the first and the last - were added into histograms. For ATP hydrolysis conditions in the presence of 1 mM ATP, the mean dwell time for *c*-ring rotation was 13±1 ms (Fig. S5A, monoexponential decay fit). Adding 20 µm aurovertin B slowed down rotation prolonging dwell times to 19±1 ms (Fig. S5B) as observed previously (Johnson et al, 2009). Fitting the broadened histogram with two exponentials resulted a rising time component of 6 ms and a decay component of 18 ms. Taking both components together, aurovertin B reduced the rotational speed by a factor of 2, or the remaining activity to ~ 50% which is in agreement with biochemical measurements. The percentage of rotating F_oF_1 was affected accordingly and reduced to about 50% (summarized in Table II below).

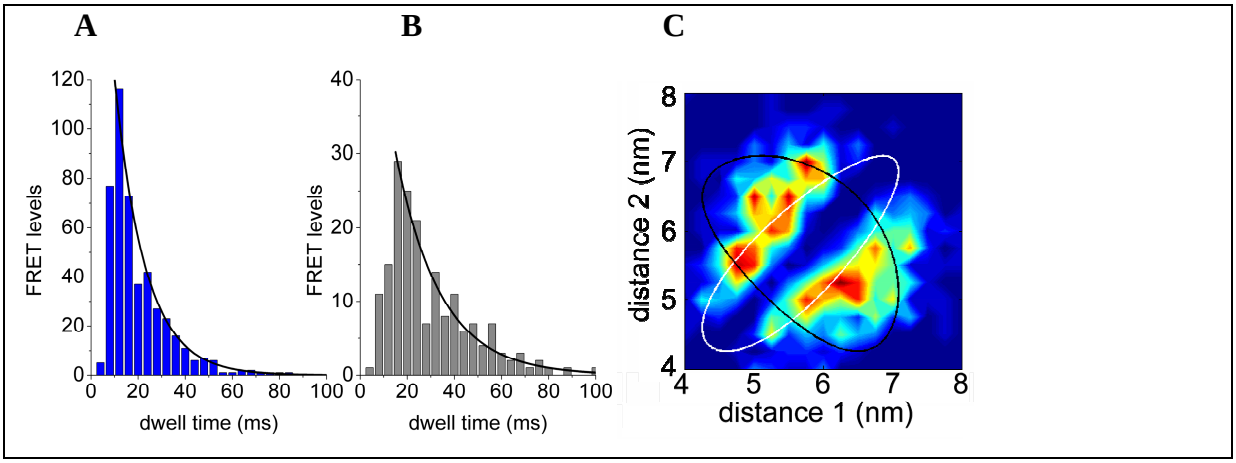

Figure S5: Dwell time histograms for *c*-ring rotation during ATP hydrolysis. **A**, in the presence of 1 mM ATP; **B**, after addition of 20 µM aurovertin B. **C**, experimental FRET transition density plot for 912 transitions during ATP hydrolysis (white curve, expected transitions for 36° stepping; black curve, expected transitions for 120° stepping of the *c*-ring).

6. FRET level statistics and classification procedures

We used two different types of single-molecule FRET measurements to determine the step size of *c*-ring rotation using the same FRET-labeled F_oF_1-ATP synthase preparation under various biochemical conditions.

To build the FRET transition density plot in Fig. 3F of the manuscript, a very large data set was required and continuous-wave laser excitation with 488 nm was applied to reduce photobleaching. In total, 11959 F_oF_1-ATP synthases were found in the fluorescence time trajectories upon ATP synthesis conditions. The threshold criteria were (I) a FRET donor fluorescence intensity exceeding 10 counts per ms and (II) a burst duration longer than 40 ms. Within the photon bursts, we found 3128 bursts showing FRET acceptor fluorescence applying a threshold for the proximity factor $P=I_A/(I_A+I_D) > 0.1$ with I_A, background-corrected fluorescence intensity of the FRET acceptor, and I_D, background-corrected fluorescence intensity of the FRET donor. This reduced number is due to the substoichiometric labeling of the *c*-ring. Within these FRET-labeled bursts, we marked FRET levels with a minimum dwell of 4 ms, a minimum count rate of 50 photons in both detection channels, and a maximum standard deviation for the proximity factor $P < 0.15$ for each FRET level. Using the given threshold criteria for an objective FRET level assignment in the manually marked fluorescence time trajectories, we obtained many photon bursts that exhibited time gaps with non-marked FRET levels. Overseen or un-assigned FRET levels appear as deviations from the ideal curve of a purely 36° *c* subunit stepping in the FRET transition density plot. The FRET transition density plot shown as Fig 3 F was build with 1879 FRET level pairs from 430 FRET-labeled F_oF_1-ATP synthases showing 2 and more FRET levels.

Similarly we analyzed FRET-labeled F_oF_1-ATP synthases in the presence of 60 µm DCCD upon ATP synthesis conditions and during ATP hydrolysis in the presence of 1 mM ATP. The numbers of FRET levels are summarized in Table I.

Biochemical condition	number of all detected F_oF_1	number of FRET-labeled F_oF_1 (percentage of all bursts)	bursts with 2 and more FRET levels (percentage of FRET bursts)	bursts with 3 and more FRET levels (percentage of FRET bursts)	FRET level pairs used for the FRET transition dens. plot (Fig. 3F)
ATP synthesis	11959	3128 (*26%*)	430 (13.7 %)	331 (10.6 %)	1879
ATP synthesis plus 60 µM DCCD	2349	524 (*22%*)	27 (5.2%)	-	-
ATP hydrolysis	5775	1222 (*21%*)	105 (8.6%)	-	-

Table I: Summary of selected photon bursts, FRET-labeled F_oF_1 and FRET levels for the single-molecule FRET transition density plot (Fig 3F) using continuous-wave laser excitation at 488 nm.

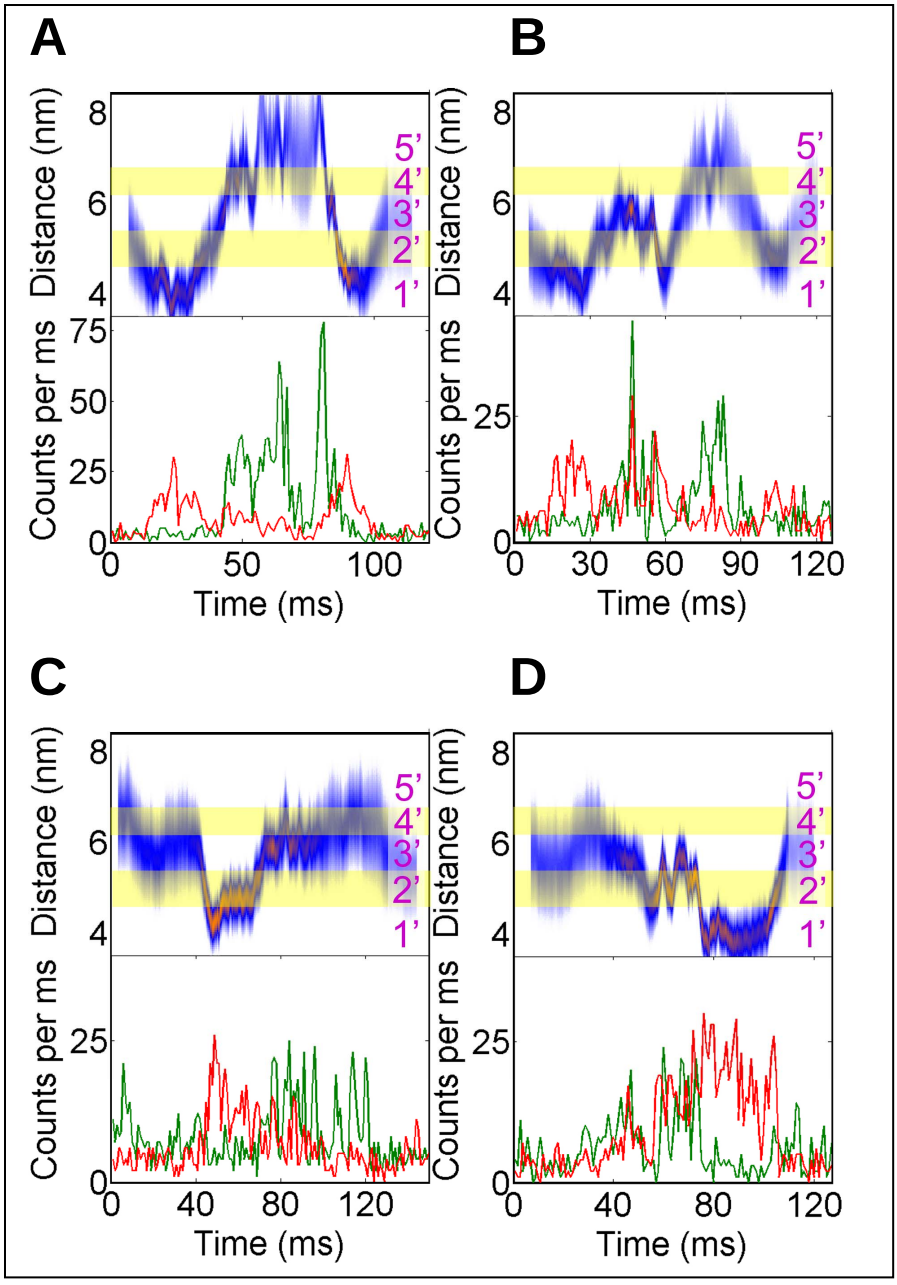

Figure S6: Photon bursts of single F_oF_1-ATP synthases using continuous-wave excitation at 488 nm. **A, B** photon bursts during ATP synthesis; **C**, **D** photon bursts during ATP hydrolysis. The five FRET distance zones were defined in Fig. 3A-C in the manuscript according to the geometrical constraints for *c*-ring rotation (1': 4.1 - 4.6 nm; 2': 4.6 - 5.4 nm, 3': 5.4 - 6.2 nm, 4': 6.2 - 6.8 nm, 5': 6.6 - 7.3 nm). Distance zones 2' and 4' are highlighted in yellow for improved perceptibility.

To control the photophysical behaviour of the EGFP fluorophore at the *a* subunit and to build the dwell time histograms in the absence and presence of the inhibitor aurovertin B, we used pulsed alternating laser excitation with 488 nm and 561 nm as described above. Photon bursts were selected by applying thresholds for a minimum count rate of the directly exited FRET acceptor fluorophore (≥ 5 counts per ms), a minimum mean intensity of 10 counts per ms in

each FRET detection channel, and a minimum duration of 40 ms for the photon burst. Five FRET data sets were obtained and are summarized in Table II.

Biochemical condition	number of bursts of FRET-labeled F_oF_1	bursts with 2 and more FRET levels (percentage of FRET bursts)	bursts with 3 and more FRET levels (percentage of FRET bursts)	FRET levels used for dwell time histograms (Fig. 2E, F, and S5A, B)
ATP hydrolysis	2229	400 (17.9 %)	208 (9.3%)	873
ATP hydrolysis in the presence of aurovertin B	2617	342 (13.1%)	125 (4.8%)	431
AMPPNP (1 mM)	1448	36 (2.5%)	4 (0.3%)	-
ATP synthesis	1058	315 (29.8%)	220 (20.8%)	998
ATP synthesis in the presence of aurovertin B	1023	80 (7.8%)	40 (3.9%)	148

Table II: Summary of the selected photon bursts and FRET levels for the single-molecule FRET analysis of dwell times using duty cycle-optimized pulsed alternating laser excitation.

In the presence of the non-hydrolysable ATP derivative AMPPNP, the number of rotating F_oF_1 was nearly abolished. This excludes any photophysical effects of EGFP as the source of the small FRET efficiency changes observed during ATP synthesis and ATP hydrolysis.

To built the FRET level transition density plot shown in Fig. S5C upon ATP hydrolysis conditions, we used the 400 photon bursts with 2 and more FRET levels yielding 912 FRET level pairs.